scientific reports

Check for updates

OPEN

Genome-wide association and multi-omics analyses provide insights into the disease mechanisms of central serous chorioretinopathy

Yuki Mori[1,2,24], Elon H. C. van Dijk[3,24], Masahiro Miyake[1,2]✉, Yoshikatsu Hosoda[4], Anneke I. den Hollander[5], Suzanne Yzer[6], Akiko Miki[7], Li Jia Chen[8], Jeeyun Ahn[9,10], Ayako Takahashi[1], Kazuya Morino[1,2], Shin-ya Nakao[1,2], Carel B. Hoyng[6], Danny S. C. Ng[8], Ling-Ping Cen[11], Haoyu Chen[11], Tsz Kin Ng[11], Chi Pui Pang[8,11], Kwangsic Joo[9,12], Takehiro Sato[13], Yasuhiko Sakata[14], Atsushi Tajima[13], Yasuharu Tabara[2,15], The Nagahama Study Group*, Kyu Hyung Park[9,16], Fumihiko Matsuda[2], Kenji Yamashiro[17], Shigeru Honda[18], Masao Nagasaki[2,19], Camiel J. F. Boon[3,20,25] & Akitaka Tsujikawa[1,25]

Central serous chorioretinopathy (CSC) is a major cause of vision loss, especially in middle-aged men, and its chronic subtype can lead to legal blindness. Despite its clinical importance, the underlying mechanisms of CSC need further clarification. In this study, we conducted a meta-analysis of three genome-wide association studies (GWASs) for CSC consisting of 8811 Asians and Caucasians, followed by replication in an additional 4338 Asians. We identified four genome-wide hits, including a novel hit (rs12960630 at *LINC01924-CDH7*, $P_{meta} = 2.97 \times 10^{-9}$). A phenome-wide association study for rs12960630 showed a positive correlation between its CSC risk allele with plasma cortisol concentration. Expression/splicing quantitative trait loci (QTL) analyses showed an association of all these hits with the expression and/or splicing of genes in genital organs, which may explain the sex differences in CSC. Protein QTL also suggested the protein-level contribution of the complement factor H pathway to CSC pathogenesis.

Abbreviations

[1]Department of Ophthalmology and Visual Sciences, Kyoto University Graduate School of Medicine, 54 Shogoin-kawahara, Sakyo, Kyoto 606-8507, Japan. [2]Center for Genomic Medicine, Graduate School of Medicine, Kyoto University, Kyoto, Japan. [3]Department of Ophthalmology, Leiden University Medical Center, Leiden, The Netherlands. [4]Hosoda Eye Clinic, Nishinomiya, Japan. [5]Genomics Research Center, Abbvie, Cambridge, MA, USA. [6]Department of Ophthalmology, Radboud University Medical Centre, Nijmegen, The Netherlands. [7]Division of Ophthalmology, Department of Surgery, Kobe University Graduate School of Medicine, Kobe, Japan. [8]Department of Ophthalmology and Visual Sciences, The Chinese University of Hong Kong, Hong Kong, China. [9]Seoul National University, College of Medicine, Seoul, Korea. [10]SMG-SNU Boramae Medical Center, Seoul, Korea. [11]Joint Shantou International Eye Center of Shantou University and The Chinese University of Hong Kong, Shantou, China. [12]Seoul National University Bundang Hospital, Seongnam, Korea. [13]Department of Bioinformatics and Genomics, Graduate School of Advanced Preventive Medical Sciences, Kanazawa University, Kanazawa, Japan. [14]Department of Clinical Medicine and Development, National Cerebral and Cardiovascular Center, Suita, Japan. [15]Graduate School of Public Health, Shizuoka Graduate University of Public Health, Shizuoka, Japan. [16]Seoul National University Hospital, Seoul, Korea. [17]Department of Ophthalmology and Visual Science, Kochi Medical School, Kochi University, Nankoku, Japan. [18]Department of Ophthalmology and Visual Sciences, Osaka Metropolitan University Graduate School of Medicine, Osaka, Japan. [19]Division of Biomedical Information Analysis, Medical Research Center for High Depth Omics, Medical Institute of Bioregulation, Kyushu University, Fukuoka, Japan. [20]Department of Ophthalmology, Amsterdam University Medical Centers, Amsterdam, The Netherlands. [24]Yuki Mori and Elon H. C. van Dijk contributed equally to this work. [25]Camiel J. F. Boon and Akitaka Tsujikawa jointly supervised this work. *A list of authors and their affiliations appears at the end of the paper. ✉email: miyakem@kuhp.kyoto-u.ac.jp

AMD	Age-related macular degeneration
CEU	Utah Residents from North and West Europe
CHART-2	Chronic Heart Failure Analysis and Registry in the Tohoku District 2
CI	Confidence interval
CSC	Central serous chorioretinopathy
eQTL	Expression QTL
EyeGEx	Eye Genotype Expression
GTEx	Genotype-tissue expression
GWAS	Genome-wide association study
HGNC	Human Genome Organization Gene Nomenclature Committee
JPT	Japanese in Tokyo, Japan
LD	Linkage disequilibrium
LDSC	LD score regression
lncRNA	Long non-coding RNA
MAF	Minor allele frequency
MNV	Macular neovascularization
NES	Normalized effect size
OCT	Optical coherence tomography
OR	Odds ratio
PC	Principal component
PheWAS	Phenome-wide association study
PP	Posterior probability
pQTL	Protein QTL
QTL	Quantitative trait loci
RNA	Ribonucleic acid
SE	Standard error
SNP	Single nucleotide polymorphism
sQTL	Splicing QTL
SYT2	Synaptotagmin-2

Central serous chorioretinopathy (CSC) is characterized by a serous retinal detachment of the macula. It is one of the common causes of vision loss and predominantly occurs in middle-aged men[1]. Many CSC cases resolve spontaneously within three months; therefore, the visual prognosis of CSC was thought to be good. However, a recent study reported that chronic CSC cases lasting ≥ 6 months had relatively poor visual prognosis, where 12.8% of cases had developed legal blindness after a mean follow-up of 11.3 years[2]. In addition, accumulating evidence relates CSC to wet age-related macular degeneration (AMD), which is one of the leading causes of irreversible blindness in developed countries[3–7]. For example, we have identified multiple genetic relationships between AMD and CSC through meta-analysis of genome-wide association studies (GWASs) for AMD[3] or genome-wide survival analysis[4]. Genetic colocalization between CSC and AMD has also been reported[3]. As such, CSC demands much attention for its clinical consequences.

Four GWASs have been conducted for CSC. The first study, conducted in 2018, evaluated 4098 Europeans and identified one genome-wide significant hit at *CFH* (i.e., *complement factor H*)[8]. The second, also in 2018[9], evaluated 1,311 Japanese individuals and identified *SLC7A5* as a novel susceptibility gene. The third study, conducted in 2019, evaluated 3,460 Japanese individuals and identified *TNFRSF10A* and *GATA5*[10]. Lastly, the 2023 meta-GWAS replicated the significance of *CFH* and *GATA5* and identified three novel susceptibility loci (*CD34/CD46*, *NOTCH4*, and *PREX1*), using two biobank-based cohorts and the aforementioned European GWAS[11].

In the current study, we meta-analyzed data from the first three GWASs together to identify the multiracial genetic backgrounds of CSC at a higher level of evidence. This is the first study to integrate CSC GWAS datasets across multiple populations, aiming to understand the genetic background shared across different ethnic groups. The meta-GWAS comprised a total of 8811 individuals and the hits were replicated in an additional 4338 Asian samples. This meta-analysis successfully identified one novel hit, which was identified to be associated with four blood molecules, including plasma cortisol, through the subsequent phenome-wide association analysis (PheWAS). Additionally, this novel hit was found to have a differential effect on CSC risk between males and females, with a greater impact observed in males, as revealed by genotype-sex interaction analysis. Furthermore, through single-tissue expression/splicing quantitative trait loci (eQTL/sQTL) analysis and protein quantitative trait loci (pQTL) analysis, we identified the possible reason for the sex differences and the protein-level contribution of the complement factor H pathway in CSC.

Results

Discovery meta-GWAS

The characteristics of the three GWAS datasets are summarized in Supplementary Table 1. A total of 4,860,401 single nucleotide polymorphisms (SNPs) from 7,543 individuals, including 1,268 patients with CSC, were meta-analyzed. Figure 1 depicts the Manhattan plot of the results. The inflation factor (λ_{GC}) was 1.154. The quantile–quantile plot is shown in Supplementary Fig. 1.

We identified a genome-wide significant association for seven loci. Four of these loci were novel; rs822602 at *NFU1P2-LINC01776* (odds ratio [OR] = 0.88 [95% confidence interval [CI], 0.84–0.92], $P = 4.41 \times 10^{-8}$), rs12032663 at *RPL39P10-CHRM3* (odds ratio [OR] = 1.09 [95% CI, 1.06–1.13], $P = 6.92 \times 10^{-9}$), rs59611893 at *MROH5* (OR = 0.92 [95% CI, 0.89–0.94], $P = 4.98 \times 10^{-9}$), rs2418196 at *RNU6-710P-SUSD1* (OR = 0.92 [95% CI,

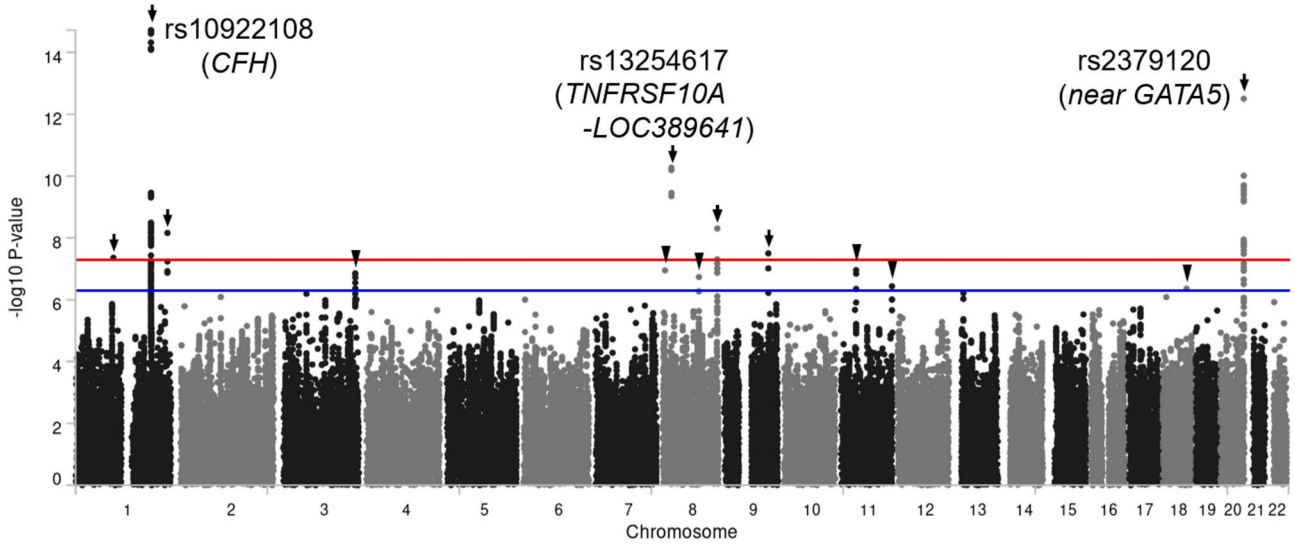

Fig. 1. Manhattan plots of the discovery stage of the genome-wide meta-analysis for central serous chorioretinopathy (CSC). The plots represent the $-\log_{10}$ transformed *P*-values for all single nucleotide polymorphisms. The *red* and *blue horizontal lines* represent the genome-wide significant threshold ($P = 5.0 \times 10^{-8}$) and the suggestive threshold ($P = 5.0 \times 10^{-7}$), respectively. Seven loci (*arrows*), including previously reported susceptibility loci for CSC (*CFH*, *TNFRSF10A-TNFRSF10A-DT*, and near *GATA5*) associate with CSC genome-wide significantly, and six loci (*arrowheads*) associate with CSC suggestively.

0.89–0.95], $P = 3.17 \times 10^{-8}$). The remaining three loci were previously reported; rs10922108 at *CFH* (OR = 0.89 [95% CI, 0.86–0.91], $P = 1.91 \times 10^{-15}$), rs13254617 at *TNFRSF10A-DT* (OR = 1.10 [95% CI, 1.07–1.14], $P = 5.38 \times 10^{-11}$), and rs2379120 near *GATA5* (OR = 0.89 [95% CI, 0.86–0.92], $P = 3.15 \times 10^{-13}$). We also identified suggestive associations for six novel loci. Of the lead SNPs of the 13 loci (summarized in Table 1), we carried 10 novel candidate SNPs forward to the replication stage. Supplementary Table 2 summarizes the results of the SNPs that showed suggestive associations ($P < 5.0 \times 10^{-7}$) with CSC.

Additionally, we looked up previously-reported CSC susceptibility SNPs using the results from the three discovery datasets and our discovery meta-GWAS (summarized in Supplementary Table 3). Of the 22 SNPs at 15 loci, results for 16 SNPs were included in our discovery meta-GWAS. For the remaining six SNPs, we examined the results of proxy SNPs with linkage disequilibrium (LD) $r^2 \geq 0.8$, and only rs1061170 at *CFH* had a proxy SNP (rs10754199, LD $r^2 = 1.00$) included in the results. Among these 17 SNPs, the only one that was not located in a suggestive or genome-wide significant locus in the discovery meta-GWAS but showed a nominally significant association was rs10490924 at *ARMS2* (effect allele/non-effect allele: T/G, Z-score = − 1.96, $P = 0.050$). For the 23 SNPs (22 previously reported SNPs and the aforementioned proxy SNP), all results were available in the Netherlands dataset. In the Kyoto and Kobe datasets, results were available for 20 SNPs, excluding rs882198 near *CD34/CD46*, rs61758735 at *PTPRB*, and rs35770820 at *PREX1*. Although rs8192569 was not replicated in either of the two Japanese datasets (both $P > 0.05$), it showed a significant association in the Netherlands dataset (OR [95% CI] = 0.65 [0.55–0.78], $P = 1.03 \times 10^{-6}$).

We mapped 780 SNPs (338 candidate SNPs of the genome-wide meta-analysis and 442 SNPs in the reference panel in strong LD with any of independent significant SNPs) to 21 candidate genes in 13 genomic loci using positional mapping (summarized in Supplementary Table 4). Of these 21 genes, 20 (excluding *FAM92A1*) were included in the database of the Human Genome Organization Gene Nomenclature Committee (HGNC) and used for functional enrichment analysis by ToppFun function of ToppGene. A total of 26 *CFH*- or *CFHR*s-related pathways showed significant associations (summarized in Supplementary Table 5).

Replication and overall meta-analysis

The characteristics of the three replication datasets are summarized in Supplementary Table 1, while Table 2 shows the results of the replication stage. After meta-analyzing the three replication datasets, one newly detected SNP, rs12960630, revealed a statistically significant association after multiple testing corrections (OR = 0.79 [95% CI, 0.67–0.93], $P = 0.004$). This SNP displayed a consistent "direction of effect" in each discovery and replication dataset.

The results of the meta-analysis of all the discovery and replication datasets are outlined in Table 2. Rs12960630 at *LINC01924-CDH7* was genome-wide significantly associated with CSC (OR = 0.77 [95% CI, 0.70–0.84], $P = 2.97 \times 10^{-9}$). Supplementary Figs. 2 and 3 present the regional association and the forest plots, respectively, for rs12960630 at *LINC01924-CDH7*.

Ethnicity-stratified analysis

To investigate differences in the genetic background of CSC between ethnicities, we compared the meta-GWAS results of two Japanese datasets (the Kyoto CSC cohort and the Kobe CSC dataset, referred to as the Japanese

Locus Number*	SNP	Position	EA/NonEA	Gene	Kyoto (CSC 610 vs. Control 2,850)		Kobe (CSC 137 vs. Control 1,116)		The Netherlands (CSC 521 vs. Control 3,577)		Meta-analysis (CSC 1,268 vs. Control 7,543)	
					OR (95% CI)	*P*-value	OR (95% CI)	*P*-value	OR (95% CI)	*P*-value	Z-score	*P*-value
1	rs822602	1:98,669,164	A/C	*NFU1P2-LINC01776*	0.64 (0.54–0.76)	2.56×10^{-7}	0.98 (0.64–1.49)	9.14×10^{-1}	0.53 (0.37–0.77)	1.17×10^{-3}	−5.47	4.41×10^{-8}
2	rs10922108	1:196,701,473	A/T	*CFH*	0.79 (0.69–0.90)	2.91×10^{-4}	0.68 (0.53–0.87)	2.51×10^{-3}	0.64 (0.56–0.73)	3.13×10^{-11}	−7.95	1.91×10^{-15}
3	rs12032663	1:239,463,126	T/C	*RPL39P10-CHRM3*	1.42 (1.23–1.64)	1.29×10^{-6}	1.51 (1.14–1.99)	3.78×10^{-3}	1.21 (1.04–1.41)	1.41×10^{-2}	5.79	6.92×10^{-9}
4	rs13060976†	3:188,199,525	C/G	*LPP*	0.68 (0.59–0.79)	4.05×10^{-7}	0.73 (0.55–0.98)	3.30×10^{-2}	0.84 (0.70–1.01)	5.80×10^{-2}	−5.26	1.43×10^{-7}
4	rs13067162	3:188,200,642	A/G	*LPP*	0.68 (0.58–0.79)	2.86×10^{-7}	0.73 (0.55–0.97)	3.24×10^{-2}	0.84 (0.70–1.01)	6.64×10^{-2}	−5.26	1.41×10^{-7}
5	rs2442622	8:6,377,330	A/T	*MCPH1*	1.42 (1.22–1.66)	7.58×10^{-6}	1.17 (0.88–1.56)	2.72×10^{-1}	1.45 (1.13–1.85)	2.15×10^{-3}	5.31	1.13×10^{-7}
6	rs13254617	8:23,083,836	A/C	*TNFRSF10A-DT*	1.37 (1.20–1.57)	2.96×10^{-6}	1.22 (0.94–1.57)	1.31×10^{-1}	1.37 (1.19–1.57)	6.98×10^{-6}	6.56	5.38×10^{-11}
7	rs11995221	8:94,667,346	A/G	*LINC00535*	1.40 (1.22–1.60)	8.80×10^{-7}	1.02 (0.78–1.34)	8.85×10^{-1}	1.24 (1.08–1.42)	2.19×10^{-3}	5.22	1.84×10^{-7}
8	rs59611893	8:142,481,511	T/C	*MROH5*	0.71 (0.62–0.81)	2.40×10^{-7}	0.94 (0.73–1.22)	6.52×10^{-1}	0.77 (0.67–0.89)	3.27×10^{-4}	−5.85	4.98×10^{-9}
8	rs12547980‡	8:142,488,837	A/G	*MROH5*	0.69 (0.61–0.79)	8.37×10^{-8}	0.93 (0.72–1.21)	6.02×10^{-1}	0.83 (0.72–0.95)	6.52×10^{-3}	−5.40	6.74×10^{-8}
9	rs2418196	9:114,798,294	A/C	*RNU6-710P-SUSD1*	0.68 (0.60–0.78)	3.66×10^{-8}	0.89 (0.68–1.16)	3.93×10^{-1}	0.83 (0.73–0.96)	9.41×10^{-3}	−5.53	3.17×10^{-8}
10	rs4756575	11:40,121,464	A/T	*LOC100421559-LINC01499*	1.45 (1.23–1.70)	6.77×10^{-6}	1.34 (0.97–1.84)	7.58×10^{-2}	1.56 (1.11–2.19)	7.43×10^{-3}	5.31	1.10×10^{-7}
11	rs6590725	11:133,534,203	T/C	*OPCML-LINC02743*	0.71 (0.61–0.83)	1.22×10^{-5}	0.74 (0.54–1.00)	4.98×10^{-2}	0.84 (0.72–0.97)	1.81×10^{-2}	−5.09	3.68×10^{-7}
12	rs12960630	18:62,695,983	A/C	*LINC01924-CDH7*	0.71 (0.61–0.82)	6.36×10^{-6}	0.85 (0.64–1.13)	2.67×10^{-1}	0.80 (0.68–0.94)	7.90×10^{-3}	−5.05	4.39×10^{-7}
13	rs2379120	20:61,030,580	A/T	*RBBP8NL-GATA5*	0.75 (0.65–0.86)	5.54×10^{-5}	0.57 (0.42–0.77)	2.60×10^{-4}	0.67 (0.57–0.79)	7.14×10^{-7}	−7.29	3.15×10^{-13}

Table 1. Summary of central serous chorioretinopathy (CSC)-associated single nucleotide polymorphisms (SNPs) in the discovery stage of the genome-wide meta-analysis. *EA* effect allele, *NonEA* non-effect allele, *OR* odds ratio, *CI* confidence interval. *Index of the assigned genomic locus matched with Supplementary Table 4. †Proxy SNP (linkage disequilibrium [LD] $r^2 = 0.99$) of the lead SNP, rs13067162, which was carried forward to the replication stage. ‡Proxy SNP (LD $r^2 = 0.82$) of the lead SNP, rs59611893, which was carried forward to the replication stage.

meta-GWAS dataset) with the GWAS results of the Netherlands CSC dataset (referred to as the European GWAS dataset). The Japanese meta-GWAS dataset included 4,989,727 SNPs from 4713 individuals, including 747 CSC patients.

The results of gene mapping for the Japanese meta-GWAS and European GWAS datasets are summarized in Supplementary Table 4. For the Japanese meta-GWAS dataset, we mapped 415 SNPs (283 candidate SNPs from the genome-wide meta-analysis and 132 SNPs in strong LD with any independent significant SNPs in the reference panel) to 9 candidate genes across 18 genomic loci. For the European GWAS dataset, we mapped 306 SNPs (178 candidate SNPs from the genome-wide meta-analysis and 129 SNPs in strong LD with any independent significant SNPs in the reference panel) to 6 candidate genes within one genomic locus. All these 6 genes were also mapped in the discovery meta-GWAS.

In the functional enrichment analysis, for the Japanese meta-GWAS dataset, all nine mapped genes were analyzed by ToppGene. However, no pathway showed a significant association with the Japanese meta-GWAS results. For the European GWAS dataset, all six mapped genes were analyzed by ToppGene, and 26 *CFH*- or *CFHR*s-related pathways showed significant associations, all of which were also significantly associated with the discovery meta-GWAS. When combining all genes mapped from both the discovery meta-GWAS and the Japanese meta-GWAS, only the same 26 pathways demonstrated significant associations. Results for these pathways are summarized in Supplementary Table 5.

Genotype-sex interactions of CSC susceptibility SNPs

Using the Kyoto CSC cohort dataset, we examined the interaction between genotype and sex for the four SNPs that showed genome-wide significance. Since control group of the dataset included participants with unknown sex (1,656 cases), we inferred sex using PLINK, successfully identifying the sex of 1,639 cases. As a result, a total of 3,443 individuals (610 patients with CSC and 2,833 controls) were included in the analysis. Among the four SNPs, two exhibited a significant genotype-sex interaction effect; rs13254617 at *TNFRSF10A-DT* (OR = 0.66 [95% CI, 0.48–0.91], $P = 0.011$), and rs12960630 at *LINC01924-CDH7* (OR = 0.64 [95% CI, 0.44–0.92], $P = 0.016$). This result indicates that the risk alleles for both SNPs have significantly lower odds ratios in females compared to males. The results for all four SNPs are summarized in Supplementary Table 6.

Multi-omics analysis

Results of the single-tissue eQTL and sQTL analyses of the four CSC susceptibility SNPs are shown in Supplementary Table 7. All four SNPs significantly altered the expression or splicing levels of at least one gene in genital organs (testis, prostate, and/or ovary). The newly identified susceptibility SNP, rs12960630, was significantly associated with the splicing of long non-coding ribonucleic acid (lncRNA) *AC007948.1* in single-tissue sQTL of the testis (normalized effect size [NES] = 0.51, $P = 7.8 \times 10^{-7}$, Supplementary Fig. 4). It should be noted that *AC007948.1* showed testis-specific expression (Supplementary Fig. 5). Additionally, we used the Eye Genotype Expression (EyeGEx) database[12] to explore retina-specific eQTL associations. However, no significant hits were identified in this analysis.

For rs10922108, six proteins—CFH, CFHR1, CFHR2, CFHR3, CFHR4, and CFHR5—were measured in the Icelander pQTL analysis[13]. Of the six proteins, CFH, CFHR1, CFHR2, CFHR3, and CFHR4 reached the significance threshold in their analysis ($P < 1.8 \times 10^{-9}$)[13] (Table 3). In the validation pQTL study for Japanese, instead of rs10922108, we evaluated the results for its direct genotyping proxy SNP, rs1329428, at *CFH* (LD $r^2 = 0.99$). The SNP was confirmed to be associated with protein expressions of CFH, CFHR2, and CFHR4 ($P = 1.41 \times 10^{-9}$, 6.09×10^{-24}, and 1.06×10^{-28}, respectively). For the other three lead SNPs, related proteins were not measured in the proteome analyses.

Potential regulation

For the four lead SNPs rs10922108, rs2379120, rs13254617, and rs12960630, 19, 13, 2, and 0 SNPs, respectively, were reported as high LD in the HaploReg database (Supplementary Table 8). Combined with the results for the proxy SNPs, all these four lead SNPs were predicted to alter the binding state of multiple motifs; three lead SNPs, i.e., rs10922108, rs2379120, and rs13254617, were located in enhancer histone marks, while rs13254617 was located in promoter histone marks.

PheWAS

Through PheWAS using the IEU OpenGWAS database (https://gwas.mrcieu.ac.uk/, accessed on July 5, 2022)[14,15], we found that the novel hit rs12960630 at *LINC01924-CDH7* was significantly associated with four phenotypes regarding blood molecules[16–19], including plasma cortisol ($\beta = -0.067$, standard error [SE] = 0.017, $P = 1.03 \times 10^{-4}$) and synaptotagmin-2 (SYT2; $\beta = -0.111$, SE = 0.032, $P = 6.17 \times 10^{-4}$). Supplementary Table 9 summarizes the four phenotypes.

Mendelian randomization (MR) analysis

The MR analyses were conducted to investigate the causal relationships between the blood molecules (as exposures) and the onset of CSC (as the outcome) by using genome-wide significant SNPs reported for each blood molecule (summarized in Supplementary Table 10). For serum total cholesterol, as only the summary data were available and lead SNPs were not explicitly reported, we identified genome-wide significantly associated genomic loci using SNP2GENE function of FUMA. The settings were partially modified from those described in Supplementary Table 11: the "Reference panel population" was set to "1000G Phase3 EUR" (i.e. European in the 1000 Genomes Project (phase3)), and "Maximum P-value of lead SNPs (<)" (i.e. genome-wide significance threshold) was set to 2.3×10^{-9}, following the criteria of the original study. For each detected genomic locus, the lead SNP with the lowest *P*-value was selected for the MR analysis. Since no genome-wide significant

Locus Number*	SNP	Position	EA/NonEA	Gene	Replication								Meta-analysis of discovery and replications (CSC 2,157 vs. Control 10,992)	
					Meta-analysis of Japan, Hong Kong, and Shantou (CSC 889 vs. Control 3,449)		Japan (CSC 353 vs. Control 1,411)		Hong Kong (CSC 222 vs. Control 1,033)		Shantou (CSC 314 vs. Control 1,005)			
					OR (95% CI)	*P*-value	OR (95% CI)	*P*-value	OR (95% CI)	*P*-value	OR (95% CI)	*P*-value	OR (95% CI)	*P*-value
1	rs822602	1:98,669,164	A/C	*NFU1P2-LINC01776*	0.99 (0.82–1.19)	0.895	0.99 (0.75–1.30)	0.925	1.19 (0.86–1.64)	0.300	0.71 (0.46–1.10)	0.121	0.76 (0.68–0.85)	3.08×10^{-6}
3	rs12032663	1:239,463,126	T/C	*RPL39P10-CHRM3*	0.95 (0.81–1.12)	0.544	0.93 (0.75–1.16)	0.526	0.99 (0.73–1.33)	0.931	0.95 (0.63–1.44)	0.820	1.22 (1.12–1.33)	2.36×10^{-6}
4	rs13060976	3:188,199,525	C/G	*LPP*	1.06 (0.90–1.25)	0.496	1.36 (1.07–1.73)	0.011	0.81 (0.61–1.08)	0.148	0.89 (0.60–1.31)	0.549	0.82 (0.75–0.90)	1.74×10^{-5}
5	rs2442622	8:6,377,330	A/T	*MCPH1*	0.91 (0.77–1.07)	0.245	0.94 (0.74–1.20)	0.623	0.96 (0.73–1.26)	0.768	0.71 (0.47–1.08)	0.105	1.20 (1.09–1.32)	2.53×10^{-4}
7	rs11995221	8:94,667,346	A/G	*LINC00535*	1.08 (0.93–1.25)	0.304	0.97 (0.80–1.19)	0.800	1.14 (0.88–1.47)	0.317	1.38 (0.94–2.02)	0.098	1.22 (1.13–1.32)	3.05×10^{-7}
8	rs12547980	8:142,488,837	A/G	*MROH5*	0.97 (0.84–1.12)	0.683	1.00 (0.82–1.23)	0.976	0.98 (0.77–1.25)	0.858	0.87 (0.61–1.23)	0.426	0.83 (0.77–0.89)	8.35×10^{-7}
9	rs2418196†	9:114,798,294	A/C	*RNU6-710P-SUSD1*	1.14 (0.90–1.44)	0.287	–	–	1.07 (0.80–1.43)	0.651	1.28 (0.85–1.91)	0.233	0.81 (0.74–0.88)	8.69×10^{-7}
10	rs4756575	11:40,121,464	A/T	*LOC100421559-LINC01499*	1.04 (0.88–1.23)	0.626	1.06 (0.82–1.37)	0.645	1.04 (0.80–1.35)	0.776	1.00 (0.68–1.48)	0.985	1.27 (1.15–1.41)	5.39×10^{-6}
11	rs6590725†	11:133,534,203	T/C	*OPCML-LINC02743*	0.95 (0.77–1.17)	0.635	–	–	1.02 (0.80–1.32)	0.853	0.82 (0.57–1.17)	0.272	0.80 (0.73–0.88)	1.53×10^{-6}
12	**rs12960630**	**18:62,695,983**	**A/C**	***LINC01924-CDH7***	**0.79 (0.67–0.93)**	**0.004**	**0.78 (0.62–0.97)**	**0.026**	**0.80 (0.59–1.08)**	**0.148**	**0.80 (0.53–1.20)**	**0.281**	**0.77 (0.70–0.84)**	$\mathbf{2.97\times10^{-9}}$

Table 2. Summary of the central serous chorioretinopathy (CSC)-associated single nucleotide polymorphisms (SNPs) in the replication stage. *EA* effect allele, *NonEA* non-effect allele, *OR* odds ratio, *CI* confidence interval. *Index of assigned genomic locus matched with Supplementary Table 4. †Results of these SNPs are unavailable in the Japan dataset because of low imputation quality ($R^2 < 0.5$). Bold: Result for SNP with genome-wide significant association in the meta-analysis of all six datasets.

Protein	EA/NonEA	Iceland (Ferkingstad et al.[19])			Japan*	
		β ($\times 10^{-1}$)	SE ($\times 10^{-1}$)	*P*-value	β ($\times 10^{-1}$)	*P*-value
CFH	T/A	1.15	0.08	4.29×10^{-44}	3.80	1.41×10^{-13}
CFHR1		−4.26	0.06	0	−0.54	0.29
CFHR2		−7.06	0.04	0	−5.15	6.09×10^{-24}
CFHR3		−0.61	0.08	2.93×10^{-14}	−0.94	0.08
CFHR4		−3.75	0.05	0	−5.69	1.06×10^{-28}
CFHR5		−0.37	0.08	6.21×10^{-6}	−0.30	0.57

Table 3. Results of protein quantitative trait loci analyses for rs10922108. *SNP* single nucleotide polymorphism, *EA* effect allele (also, risk allele for central serous chorioretinopathy), *NonEA* non-effect allele, *SE* standard error. *Data for rs1329428, the direct genotyping proxy SNP of rs10922108 (linkage disequilibrium $r^2 = 0.99$) are shown. SEs were not available.

regions were reported for SYT-2, this molecule was excluded from the analysis. No significant associations were observed using both the inverse variance weighted method and the MR Egger method (all *P*s ≥ 0.05). Similarly, no significant causal effect was found when analyzing the potential influence of CSC (as the exposure) on the levels of these blood molecules (as outcomes), using the four genome-wide significant SNPs identified in this study for CSC (all *P*s ≥ 0.05). These results are summarized in Supplementary Table 12.

Genetic colocalization between CSC and AMD

To investigate the genetic colocalization between CSC and AMD, we analyzed the results of the discovery meta-GWAS and a previously reported Japanese AMD meta-GWAS. Seven loci with genome-wide significant associations with either CSC or AMD (*CFH*, *C2-CFB*, *TNFRSF10A-TNFRSF10A-DT*, *WBP1L*, *ARMS2*, *LINC01924-CDH7*, and *RBBP8NL-GATA5*) were included in the analysis. The results are summarized in Supplementary Table 13. The analysis indicated a high probability of shared causal SNPs between CSC and AMD at the *TNFRSF10A-TNFRSF10A-DT* (posterior probability [PP] = 99.1%) and *RBBP8NL-GATA5* loci (PP = 98.3%).

Discussion

In the current study, we identified rs12960630 at *LINC01924-CDH7* as a novel susceptibility SNP for CSC via a meta-GWAS of 4713 Japanese and 4098 Europeans. This SNP was successfully replicated in 4338 Asians, and a genotype-sex interaction on CSC risk (greater in males than females) was observed. In addition, PheWAS of the SNP revealed that it was associated with four blood molecules, including plasma cortisol. Furthermore, single-tissue eQTL and sQTL analyses suggested a potential link to sex differences in CSC, and in pQTL analysis, the result suggested the protein-level contribution of the complement factor H pathway to CSC pathogenesis.

Before 2018, Several susceptibility genes for CSC have been identified through candidate gene studies[20–26]. However, most of these susceptibility genes identified through candidate gene studies have not been replicated by later GWASs. The only exception is *CFH*, which is well-replicated as a susceptibility gene for CSC. Interestingly, the same SNP of *CFH* is also an established susceptibility gene for the vision-threatening disease AMD, though the effect directions are opposite between AMD and CSC[20]. We have also identified three additional susceptibility genes for CSC through two GWASs. An intermediate phenotype (i.e., choroidal thickness) two-staged GWAS of 6,110 healthy Japanese individuals, lead to the identification of *VIPR2*[25], *TNFRSF10A*, and *GATA5*[10]. The current meta-GWAS successfully confirmed the involvement of *CFH*, *TNFRSF10A* and *GATA5*, while the contribution of other candidate SNPs was not replicated. The lack of replication for other SNPs may reflect their initial discovery in candidate gene studies or differences in population genetics.

Multi-layered QTL mapping provided important insights into the pathogenesis of CSC. In tissue-specific analyses, the SNPs most significantly associated with CSC in the three genes previously reported and replicated in this study, regulated the expression and/or splicing of several genes in genital organs. For instance, rs10922108 at *CFH* regulated the expression of *CFHR1* in testes and the expression and splicing of *CFH* in ovaries, while rs2379120 near *GATA5* regulated the splicing of *RP5-908M14.5* in testes. This is likely to contribute to the sex differences observed in CSC patients. Future studies on the pathways of these genes in different sexes are warranted. Interestingly, for *CFH*, the T allele of rs10922108 (risk allele for CSC) caused increased gene expression in organs as well as increased protein expression in plasma, whereas, for some *CFHR*s, it did not cause decreased protein expression in plasma despite decreased gene expression in organs, at least in the Japanese cohort. This suggested that the regulation of the complement factor H pathway in tissues other than the eye may also indirectly contribute to CSC development. Furthermore, the significance of complement factor H in CSC pathogenesis was underscored by functional enrichment analysis results, where *CFH*- or *CFHR*s-related pathways emerged as notably associated with CSC, further supporting role of complement factor H as a key factor in CSC. The results of HaploReg suggested that these regulations were caused by enhancer/promoter histone marks, motif alternations, and more. While our analyses focused on single-tissue eQTL, sQTL, and pQTL mapping in multiple tissue types, which enabled us to identify regulatory mechanisms potentially linked to CSC, future tissue-specific pQTL analysis is expected to elucidate the pathogenesis of CSCs in more detail. More advanced multi-omics approaches, integrating epigenomic, proteomic, and metabolomic data across

cellular and tissue contexts, could offer additional insights into CSC pathogenesis and help clarify the biological mechanisms underpinning genetic susceptibility to CSC.

The male predominance in CSC incidence is well-established, but its genetic basis concerning sex remains unclear. Our study identified significant genotype-sex interactions for *TNFRSF10A-DT* and the novel locus, *LINC019240CDH7*, where genetic effects on CSC were greater in males. However, no significant interactions were observed for *CFH* or *RBBP8NL-GATA5*. In contrast, previous study reported *CFH* variants as male-specific and *TNFRSF10A* as non-sex-specific, differing from our findings. These discrepancies may reflect population or methodological differences, highlighting the need for larger, diverse studies to clarify the genetic mechanisms underlying sex differences in CSC.

While the exact mechanisms of the novel susceptibility SNP rs12960630 remain unknown, the involvement thereof in the development of CSC is plausible based on the current PheWAS, single-tissue sQTL, and regulatory prediction analysis results. Firstly, PheWAS indicated that the C allele of the SNP associated with an increased risk of CSC was positively associated with the concentration of plasma cortisol, which is in line with the fact that corticosteroid use is a well-known risk factor for CSC[27]. Although the three SNPs used in the MR analysis, with plasma cortisol as the exposure, are thought to account for a substantial part of its estimated 30–60% heritability, they explain only < 1% of the actual variance in cortisol concentration[16]. This limited explained variance may have made it challenging for the MR analysis to detect a significant causal association. Secondly, PheWAS showed a significant association between this SNP and SYT2, a Ca^{2+} sensor mediating neurotransmitter release, which is expressed in the frontal lobe[28] and controls emotion; this may have some effect on type A personality, which is another risk factor for CSC[27]. Thirdly, the association of the SNP with the splicing of a lncRNA (*AC007948.1*) specifically expressed in testes may explain the male dominant prevalence of CSC. The functional analysis of this lncRNA can lead to a further understanding of CSC. Finally, rs12960630 is predicted to alter the binding state of six motifs, further highlighting the importance of rs12960630.

In our genetic colocalization analysis, strong evidence suggested that CSC and AMD share causal SNPs in the *TNFRSF10A-TNFRSF10A-DT* and *RBBP8NL-GATA5*, supporting previous findings[3]. While prior studies indicated the possibility of shared causal SNPs in *WBP1L* between CSC and AMD, our analysis did not find strong evidence to support this. Among the CSC susceptibility loci, the novel locus, *LINC01924-CDH7*, showed a relatively high probability of not being associated with AMD, suggesting its potential involvement in CSC-specific pathogenic mechanisms. Further investigation is warranted to enhance our understanding of the classification and pathophysiology of AMD-related diseases, including those within the pachychoroid spectrum.

This is the first multi-ethnic meta-GWAS for CSC with a large replication sample. Though there are strengths in its sample size and reproducibility, the sample size remains a limitation. Because our study could identify only one novel hit, more samples may reveal additional parts of the molecular mechanisms of CSC through GWAS. In addition, potential population structure issues were observed within the Japanese meta-GWAS, as indicated by elevated lambda GC values. Despite applying stringent quality control filters (heterogeneity $I^2 < 25\%$ and MAF ≥ 10%), these values remained high, suggesting that genetic structure within the Japanese sample may have influenced the observed results. Another limitation is that the current study did not take the most recent CSC classification into account. Recently, an updated classification for CSC was published[29], in which CSC is classified into simple and complex types according to the area of retinal pigment epithelium atrophy. Although their genetic differences have not been recognized, subtype analysis may lead to further understanding of CSC in the future.

In conclusion, this first multi-ethnic meta-GWAS of CSC identified a novel robust susceptibility SNP for CSC and confirmed the association of previously reported susceptibility SNPs. Results of single-tissue eQTL and sQTL revealed the association between these SNPs and gene regulation in genital organs, which may be of importance in explaining the sex differences in CSC. Additionally, pQTL analysis suggested the protein-level contribution of the complement factor H pathway to CSC pathogenesis. Further studies are warranted.

Methods

Ethics statement

All participants provided written informed consent. All human research was conducted according to the Declaration of Helsinki and approved by the following institutional review boards and/or medical ethics committees:

- *The Kyto CSC Cohort*: Kyoto University Graduate School and Faculty of Medicine Ethics Committee, and Institutional Review Board at the Aichi Cancer Center Research Institute, Oita University Faculty of Medicine, Nagahama City Hospital.
- *The Kobe CSC dataset*: Institutional Review Board at the Kobe University Graduate School of Medicine, Tokushima University, University of Yamanashi, Nihon University, Kyushu University, and the Aichi Cancer Center Research Institute.
- *The Netherlands dataset*: The ethics committee of Leiden University Medical Center.
- *The Japan dataset*: Kyoto University Graduate School and Faculty of Medicine Ethics Committee, the Nagahama Municipal Review Board of Personal Information Protection, and Institutional Review Board at Fukushima Medical University, Kagawa University, and University of Yamanashi.
- *The Hong Kong dataset*: The Ethics Committee on Human Research of the Chinese University of Hong Kong.
- *The Shantou dataset*: The Ethics Committee of the Joint Shantou International Eye Centre.

Discovery meta-GWAS

For the discovery stage, we meta-analyzed three GWAS datasets: the Kyoto CSC cohort (610 Japanese patients with CSC and 2,850 healthy controls), the Kobe CSC dataset (137 Japanese patients with CSC and 1,116 healthy

controls), and the Netherlands CSC dataset (521 Caucasian patients with chronic CSC and 3,577 healthy controls). The details of the datasets can be found in the respective studies[8–10]. As we included only CSC cases without macular neovascularization (MNV) at registration, the numbers of CSC cases in the Kyoto and Kobe datasets are different from previous GWASs. Genome-wide genotyping, quality checks, and association studies of the Kyoto and Kobe datasets are summarized in Supplementary Note 1, while that for the Netherlands dataset was described previously[8].

These three datasets were meta-analyzed with the sample-size-based fixed-effect model, wherein we analyzed the SNPs available in all three datasets and with heterogeneity $I^2 < 75\%$. Based on previously published methods[30], the meta-analysis β and SE were calculated using the following formulas:

$$SE = \frac{1}{\sqrt{2f\,(1-f)\,(N+Z^2)}}$$
$$\beta = Z \times SE$$

In these formulas, f denotes the minor allele frequency (MAF), N denotes the sample size, and Z denotes the Z-score. Regarding the MAF, the average of the MAFs for Japanese (Japanese in Tokyo, Japan [JPT]) and European (Utah Residents from North and West Europe [CEU]) populations was used. The ORs and 95% CIs were then calculated using β and SE.

We carried the lead SNPs of the detected genomic risk loci or their proxy SNPs with LD $r^2 \geq 0.8$ forward to the replication stage. Moreover, we investigated previously reported CSC susceptibility SNPs (summarized in Supplementary Table 3).

To detect genomic risk loci, we performed gene-mapping of the SNPs that demonstrated a nominal association ($P < 0.05$) with a MAF ≥ 1% in the discovery stage of the meta-GWAS, by using the SNP2GENE function of FUMA v1.3.6a (https://fuma.ctglab.nl/). FUMA is a commonly-used online software for genetic research[31–33] that integrates 18 biological databases and tools for processing GWAS summary statistics[34]. The detailed settings we used are described in Supplementary Table 10. We then conducted a functional enrichment analysis of the mapped genes using the ToppFun module of ToppGene (https://toppgene.cchmc.org/)[35], an established online tool that performs gene list enrichment based on functional annotations and protein interaction networks[4,36,37] We focused on three pathway categories: GO: Biological Process, GO: Cellular Component, and GO: Molecular Function. To refine our search for pathways specifically related to the mapped genes, we excluded pathways containing ≥ 50 genes. Additionally, to minimize false positives, we excluded pathways associated with only a single mapped gene.

Replication analysis

For the replication stage, we enrolled 889 patients with CSC and 3,449 healthy individuals from Japan, Hong Kong, and Shantou (a city located in southeast China). The details are described in Supplementary Note 2. Briefly, for the Japan dataset, 353 unrelated patients with CSC without MNV at registration were recruited from across Japan (Kyoto University Hospital, Kagawa University Hospital, University of Yamanashi Hospital, and the Fukushima Medical University Hospital). In addition, 1,411 unrelated healthy control individuals were recruited from the Nagahama Prospective Cohort for Comprehensive Human Bioscience (the Nagahama Study, the details are described in Supplementary Note 3). The diagnosis of CSC was made by two retina specialists and the details are described in the previous study[10]. The samples were genotyped using the Asian Screening Array, and imputation was performed using the Michigan Imputation Server. We conducted GWAS using this data adjusted for age, sex, and the 1st to 3rd principal components (PCs) and looked up SNPs of interest from the output result.

For the Hong Kong dataset, 222 unrelated patients with chronic CSC and 1,033 unrelated healthy control individuals were recruited from the Chinese University of Hong Kong Eye Centre, the Prince of Wales Hospital Eye Centre, and the Hong Kong Eye Hospital. Unrelated control subjects aged ≥ 30 years were recruited from the attendants of the clinics for unrelated eye conditions. For the Shantou dataset, 314 unrelated patients with CSC and 1,005 unrelated healthy control individuals were recruited from the Joint Shantou International Eye Centre. The inclusion criteria were the same as that in the Hong Kong cohort. The samples from the Hong Kong and Shantou datasets were genotyped using TaqMan genotyping assays (Applied Biosystems, Foster City, California) on a Roche LightCycler® 480 Real-Time PCR System (Roche, Switzerland). We conducted a logistic regression adjusting for age and sex to evaluate the association.

Finally, the results of the discovery and replication stages were meta-analyzed using a fixed-effect model.

Ethnicity-stratified analysis

To investigate differences in the genetic background of CSC between ethnicities, we compared the meta-GWAS results of two Japanese datasets (the Kyoto CSC cohort and the Kobe CSC dataset) with the GWAS results of the Netherlands CSC dataset. Two Japanese datasets were meta-analyzed with the sample-size-based fixed-effect model, wherein we analyzed the SNPs available in both datasets and with heterogeneity $I^2 < 25\%$. We analyzed SNPs that were included in both the Japanese meta-GWAS and the European GWAS. The Japanese meta-GWAS and European GWAS were processed with FUMA for gene-mapping, followed by functional enrichment analysis with ToppGene, as in the discovery meta-GWAS.

Genotype-sex interaction analysis

To examine the influence of sex on the genetic background of CSC onset, we conducted a logistic regression analysis that included an interaction term between sex and genotype for the four loci identified as genome-wide significant for CSC in this study. The Kyoto CSC cohort dataset was used for this analysis. For control

participants with unknown sex, we applied the "–check-sex" function in PLINK to infer sex, excluding cases where sex determination was unsuccessful from the analysis.

Single-tissue eQTL and sQTL analyses

To clarify the association between the CSC susceptibility SNPs and the expression of transcripts, we conducted single-tissue eQTL and sQTL analyses. For single-tissue eQTL analysis, we searched for genes whose messenger RNA levels differ by the genotypes of the CSC susceptibility SNPs in the Genotype Tissue Expression (GTEx) Portal (https://gtexportal.org/home/, Release V8 accessed on October 6, 2022), which is a comprehensive public resource of tissue-specific gene expression and regulation. For single-tissue sQTL analysis, we also searched genes whose selective splicing is affected by the genotypes of the CSC susceptibility SNPs in the GTEx Portal. Additionally, to explore retina-specific eQTLs and sQTLs, we utilized the EyeGEx dataset[12] in FUMA to search for relevant associations.

pQTL analysis

To understand the association between the SNPs and protein expression, we evaluated the large-scale pQTL study from Iceland[13] and tried to reconfirm these associations in our Japanese study. The Icelandic study measured 4719 proteins using an aptamer-based technology from 35,559 participants and applied it to the pQTL analysis. The cis-pQTL associations between the SNPs showed genome-wide significance in our study, and genes chromosomally located as their cis-related genes were evaluated with the significance threshold in the Icelandic study ($P < 1.8 \times 10^{-9}$)[13].

To reconfirm the association, as an independent study, we used the participants of the Chronic Heart Failure Analysis and Registry in the Tohoku District 2 (CHART-2) Study in Japan[38]. In the CHART-2 Study, 743 individuals had their proteomes measured using the same aptamer-based technology[39] and genotypes from a SNP Array with Japonica v2[40]. The expression of proteins was normalized by inverse normal transformation. Linear regressions were performed on genotypes of SNPs that showed genome-wide significance in our study and the normalized proteome expressions using PLINK (v2.00a3LM) with age, sex, and the 1st and 2nd PCs as covariates to obtain the beta and *P*-value.

Potential regulatory prediction analysis

Functional annotations, including enhancer histone marks and motifs, were applied to the four lead SNPs of genome-wide significance and their proxy SNPs with a high LD > 0.8 using the HaploReg v4.1 database (https://pubs.broadinstitute.org/mammals/haploreg/haploreg.php, accessed on September 26, 2022)[41].

PheWAS

We performed PheWAS using the IEU OpenGWAS database (https://gwas.mrcieu.ac.uk/, accessed on July 5, 2022)[14,15], which integrates > 42,000 GWAS summary datasets and allows a comprehensive search for phenotypes that are significantly associated ($P < 0.001$) with the SNP of interest. Using IEU OpenGWAS, we searched the result for phenotypes of blood molecules.

MR analysis

To explore potential causal relationships between the four blood molecules identified in the PheWAS and the onset of CSC, we performed MR analyses. The analyses were conducted using summary data from our discovery meta-GWAS and publicly available summary statistics for each blood molecule[16–19]. The MR analysis investigating whether each of the blood molecules (as exposures) is a causal factor for CSC (as the outcome) was conducted using genome-wide significant SNPs as reported for each blood molecule (summarized in Supplementary Table 8). Conversely, to assess whether CSC (as the exposure) acts as a causal factor for changes in these blood molecules (as outcomes), we used four SNPs identified as genome-wide significant in this study for CSC. The analyses were performed using both the inverse variance weighted method and the MR Egger method.

Genetic colocalization analysis

We analyzed the results of the discovery meta-GWAS for CSC and the previously published meta-GWAS for AMD in the Japanese population. We focused on four genomic regions significantly associated with CSC in the discovery meta-GWAS (*CFH*, *TNFRSF10A-TNFRSF10A-DT*, *LINC01924-CDH7*, *RBBP8NL-GATA5*) and six genomic regions significantly associated with AMD in the Japanese meta-GWAS (*CFH*, *C2-CFB*, *TNFRSF10A*, *ARMS2*, *WBP1L*, *RBBP8NL-GATA5*). For each region, we extended the range by ± 250 kbp upstream and downstream of the target region. For the *TNFRSF10A*-related loci, *TNFRSF10A* was included within the broader *TNFRSF10A-TNFRSF10A-DT* locus; therefore, we adopted the latter for analysis.

The analysis was conducted using the coloc package version 5.2.3 for R[42–44]. In this analysis, the following hypotheses were evaluated: H_1—Association is present with CSC but not with AMD; H_2—Association is present with AMD but not with CSC; H_3—Both CSC and AMD are associated, but they have distinct causal variants; H_4—Both CSC and AMD are associated, and they share a single causal variant.

Statistical analysis

METAL v2011-03-25 (https://genome.sph.umich.edu/wiki/METAL_Documentation)[45] was used to meta-analyze the three GWASs. METAL is a software used for genetic research that performs meta-GWAS at a high speed and on low-capacity workstations. The metafor package v3.0-2 for R[46] was used for the subsequent targeted meta-analysis.

The R 4.2.0 software (The R Foundation for Statistical Computing, Vienna, Austria) was used for statistical analysis. The MAFs for Japanese (JPT) and European (CEU) and the pair-wise measures of LD r^2 in a mixed population of Japanese (JPT) and European (CEU) in the 1000 Genomes Project dataset (phase3 v5 release) were obtained via LDlink 5.1 (https://ldlink.nci.nih.gov/?tab=home) using the LDlinkR package v1.1.2 for R[47,48]. MR analyses were conducted with the TwoSampleMR package version 0.6.4 for R[14].

A *P*-value of < 0.05 was considered statistically significant. In GWAS, a *P*-value of $< 5.0 \times 10^{-8}$ was considered genome-wide significant.

Data availability

The data that support the findings of this study are available upon reasonable request. Requests for access to the data should be sent via email to the corresponding author, Masahiro Miyake, at miyakem@kuhp.kyoto-u.ac.jp.

Received: 23 January 2024; Accepted: 26 February 2025
Published online: 17 March 2025

References

1. Cheung, C. M. G. et al. Pachychoroid disease. *Eye (Lond)* **33**, 14–33. https://doi.org/10.1038/s41433-018-0158-4 (2019).
2. Mrejen, S. et al. Long-term visual outcomes and causes of vision loss in chronic central serous chorioretinopathy. *Ophthalmology* **126**, 576–588. https://doi.org/10.1016/j.ophtha.2018.12.048 (2019).
3. Akiyama, M. et al. GWAS of age-related macular degeneration reveals two new loci implying shared genetic components with central serous chorioretinopathy. *Ophthalmology* https://doi.org/10.1016/j.ophtha.2022.10.034 (2023).
4. Mori, Y. et al. Genome-wide survival analysis for macular neovascularization development in central serous chorioretinopathy revealed shared genetic susceptibility with polypoidal choroidal vasculopathy. *Ophthalmology* **129**, 1034–1042. https://doi.org/10.1016/j.ophtha.2022.04.018 (2022).
5. Miyake, M. et al. Pachychoroid neovasculopathy and age-related macular degeneration. *Sci. Rep.* **5**, 16204. https://doi.org/10.1038/srep16204 (2015).
6. Hosoda, Y. et al. Deep phenotype unsupervised machine learning revealed the significance of pachychoroid features in etiology and visual prognosis of age-related macular degeneration. *Sci. Rep.* **10**, 18423. https://doi.org/10.1038/s41598-020-75451-5 (2020).
7. Yanagi, Y. Pachychoroid disease: A new perspective on exudative maculopathy. *Jpn. J. Ophthalmol.* **64**, 323–337. https://doi.org/10.1007/s10384-020-00740-5 (2020).
8. Schellevis, R. L. et al. Role of the complement system in chronic central serous chorioretinopathy: A genome-wide association study. *JAMA Ophthalmol.* **136**, 1128–1136. https://doi.org/10.1001/jamaophthalmol.2018.3190 (2018).
9. Miki, A. et al. Genome-wide association study to identify a new susceptibility locus for central serous chorioretinopathy in the Japanese population. *Invest. Ophthalmol. Vis. Sci.* **59**, 5542–5547. https://doi.org/10.1167/iovs.18-25497 (2018).
10. Hosoda, Y. et al. Genome-wide association analyses identify two susceptibility loci for pachychoroid disease central serous chorioretinopathy. *Commun. Biol.* **2**, 468. https://doi.org/10.1038/s42003-019-0712-z (2019).
11. Rämö, J. T. et al. Overlap of genetic loci for central serous chorioretinopathy with age-related macular degeneration. *JAMA Ophthalmol.* https://doi.org/10.1001/jamaophthalmol.2023.0706 (2023).
12. Ratnapriya, R. et al. Retinal transcriptome and eQTL analyses identify genes associated with age-related macular degeneration. *Nat. Genet.* **51**, 606–610. https://doi.org/10.1038/s41588-019-0351-9 (2019).
13. Ferkingstad, E. et al. Large-scale integration of the plasma proteome with genetics and disease. *Nat. Genet.* **53**, 1712–1721. https://doi.org/10.1038/s41588-021-00978-w (2021).
14. Hemani, G. et al. The MR-Base platform supports systematic causal inference across the human phenome. *Elife* **7**, e34408. https://doi.org/10.7554/eLife.34408 (2018).
15. Elsworth, B. et al. The MRC IEU OpenGWAS data infrastructure. bioRxiv. https://doi.org/10.1101/2020.08.10.244293 (2020).
16. Bolton, J. L. et al. Genome wide association identifies common variants at the *SERPINA6*/*SERPINA1* locus influencing plasma cortisol and corticosteroid binding globulin. *PLoS Genet.* **10**, e1004474. https://doi.org/10.1371/journal.pgen.1004474 (2014).
17. Sun, B. B. et al. Genomic atlas of the human plasma proteome. *Nature* **558**, 73–79. https://doi.org/10.1038/s41586-018-0175-2 (2018).
18. Shin, S. Y. et al. An atlas of genetic influences on human blood metabolites. *Nat. Genet.* **46**, 543–550. https://doi.org/10.1038/ng.2982 (2014).
19. Kettunen, J. et al. Genome-wide study for circulating metabolites identifies 62 loci and reveals novel systemic effects of *LPA*. *Nat. Commun.* **7**, 11122. https://doi.org/10.1038/ncomms11122 (2016).
20. Miki, A. et al. Common variants in the complement factor H gene confer genetic susceptibility to central serous chorioretinopathy. *Ophthalmology* **121**, 1067–1072. https://doi.org/10.1016/j.ophtha.2013.11.020 (2014).
21. Schubert, C. et al. Cadherin 5 is regulated by corticosteroids and associated with central serous chorioretinopathy. *Hum. Mutat.* **35**, 859–867. https://doi.org/10.1002/humu.22551 (2014).
22. Breukink, M. B. et al. Genomic copy number variations of the complement component *C4B* gene are associated with chronic central serous chorioretinopathy. *Invest. Ophthalmol. Vis. Sci.* **56**, 5608–5613. https://doi.org/10.1167/iovs.15-17343 (2015).
23. de Jong, E. K. et al. Chronic central serous chorioretinopathy is associated with genetic variants implicated in age-related macular degeneration. *Ophthalmology* **122**, 562–570. https://doi.org/10.1016/j.ophtha.2014.09.026 (2015).
24. van Dijk, E. H. C. et al. Association of a haplotype in the *NR3C2* gene, encoding the mineralocorticoid receptor, with chronic central serous chorioretinopathy. *JAMA Ophthalmol.* **135**, 446–451. https://doi.org/10.1001/jamaophthalmol.2017.0245 (2017).
25. Hosoda, Y. et al. *CFH* and *VIPR2* as susceptibility loci in choroidal thickness and pachychoroid disease central serous chorioretinopathy. *Proc. Natl. Acad. Sci. U S A* **115**, 6261–6266. https://doi.org/10.1073/pnas.1802212115 (2018).
26. Feng, L. et al. Discovery of Novel genetic risk loci for acute central serous chorioretinopathy and genetic pleiotropic effect with age-related macular degeneration. *Front. Cell Dev. Biol.* **9**, 696885. https://doi.org/10.3389/fcell.2021.696885 (2021).
27. Kaye, R. et al. Central serous chorioretinopathy: An update on risk factors, pathophysiology and imaging modalities. *Prog. Retin. Eye Res.* **79**, 100865. https://doi.org/10.1016/j.preteyeres.2020.100865 (2020).
28. Melland, H., Carr, E. M. & Gordon, S. L. Disorders of synaptic vesicle fusion machinery. *J. Neurochem.* **157**, 130–164. https://doi.org/10.1111/jnc.15181 (2021).
29. Chhablani, J. & Cohen, F. B. Multimodal imaging-based central serous chorioretinopathy classification. *Ophthalmol. Retina* **4**, 1043–1046. https://doi.org/10.1016/j.oret.2020.07.026 (2020).
30. Zhu, Z. et al. Integration of summary data from GWAS and eQTL studies predicts complex trait gene targets. *Nat. Genet.* **48**, 481–487. https://doi.org/10.1038/ng.3538 (2016).
31. Cordell, H. J. et al. An international genome-wide meta-analysis of primary biliary cholangitis: Novel risk loci and candidate drugs. *J Hepatol* **75**, 572–581. https://doi.org/10.1016/j.jhep.2021.04.055 (2021).

32. Bernabeu, E. et al. Sex differences in genetic architecture in the UK Biobank. *Nat. Genet.* **53**, 1283–1289. https://doi.org/10.1038/s41588-021-00912-0 (2021).
33. Harper, A. R. et al. Common genetic variants and modifiable risk factors underpin hypertrophic cardiomyopathy susceptibility and expressivity. *Nat. Genet.* **53**, 135–142. https://doi.org/10.1038/s41588-020-00764-0 (2021).
34. Watanabe, K., Taskesen, E., van Bochoven, A. & Posthuma, D. Functional mapping and annotation of genetic associations with FUMA. *Nat. Commun.* **8**, 1826. https://doi.org/10.1038/s41467-017-01261-5 (2017).
35. Chen, J., Bardes, E. E., Aronow, B. J. & Jegga, A. G. ToppGene Suite for gene list enrichment analysis and candidate gene prioritization. *Nucleic Acids Res.* **37**, W305-311. https://doi.org/10.1093/nar/gkp427 (2009).
36. Liu, X. et al. The complex genetics of hypoplastic left heart syndrome. *Nat Genet* **49**, 1152–1159. https://doi.org/10.1038/ng.3870 (2017).
37. Small, K. S. et al. Regulatory variants at KLF14 influence type 2 diabetes risk via a female-specific effect on adipocyte size and body composition. *Nat. Genet.* **50**, 572–580. https://doi.org/10.1038/s41588-018-0088-x (2018).
38. Ushigome, R. et al. Temporal trends in clinical characteristics, management and prognosis of patients with symptomatic heart failure in Japan—report from the CHART Studies. *Circ. J.* **79**, 2396–2407. https://doi.org/10.1253/circj.CJ-15-0514 (2015).
39. Williams, S. A. et al. A proteomic surrogate for cardiovascular outcomes that is sensitive to multiple mechanisms of change in risk. *Sci. Transl. Med.* **14**, eabj9625. https://doi.org/10.1126/scitranslmed.abj9625 (2022).
40. Kawai, Y. et al. Japonica array: improved genotype imputation by designing a population-specific SNP array with 1070 Japanese individuals. *J. Hum. Genet.* **60**, 581–587. https://doi.org/10.1038/jhg.2015.68 (2015).
41. Ward, L. D. & Kellis, M. HaploReg v4: Systematic mining of putative causal variants, cell types, regulators and target genes for human complex traits and disease. *Nucleic Acids Res.* **44**, D877–D881. https://doi.org/10.1093/nar/gkv1340 (2016).
42. Giambartolomei, C. et al. Bayesian test for colocalisation between pairs of genetic association studies using summary statistics. *PLoS Genet.* **10**, e1004383. https://doi.org/10.1371/journal.pgen.1004383 (2014).
43. Wallace, C. Eliciting priors and relaxing the single causal variant assumption in colocalisation analyses. *PLoS Genet.* **16**, e1008720. https://doi.org/10.1371/journal.pgen.1008720 (2020).
44. Wallace, C. A more accurate method for colocalisation analysis allowing for multiple causal variants. *PLoS Genet.* **17**, e1009440. https://doi.org/10.1371/journal.pgen.1009440 (2021).
45. Willer, C. J., Li, Y. & Abecasis, G. R. METAL: Fast and efficient meta-analysis of genomewide association scans. *Bioinformatics* **26**, 2190–2191. https://doi.org/10.1093/bioinformatics/btq340 (2010).
46. Viechtbauer, W. Conducting meta-analyses in r with the metafor package. *J. Stat. Softw.* **36**, 1–48. https://doi.org/10.18637/jss.v036.i03 (2010).
47. Machiela, M. J. & Chanock, S. J. LDlink: A web-based application for exploring population-specific haplotype structure and linking correlated alleles of possible functional variants. *Bioinformatics* **31**, 3555–3557. https://doi.org/10.1093/bioinformatics/btv402 (2015).
48. Myers, T. A., Chanock, S. J. & Machiela, M. J. LDlinkR: An R package for rapidly calculating linkage disequilibrium statistics in diverse populations. *Front. Genet.* **11**, 157. https://doi.org/10.3389/fgene.2020.00157 (2020).

Acknowledgements

We thank Ms. Hatsue Hamanaka and Ms. Nao Harada for their assistance in genotyping the Kyoto CSC Cohort. The GTEx Project was supported by the Common Fund of the Office of the Director of the National Institutes of Health, and by the National Cancer Institute, National Human Genome Research Institute, National Heart, Lung, and Blood Institute, National Institute of Drug Abuse, National Institute of Mental Health, and the National Institute of Neurological Disorders and Stroke.

Author contributions

Conceptualization: Y.M., M.M. Methodology: Y.M., M.M. Investigation: Y.M., M.M., Y.H., A.I.dH., S.Y., A.M., L.J.C., J.A., A.T., K.M., S.N., C.B.H., D.S.C.N., L.P.C., H.C., T.K.N., C.P.P., K.J., Y.S., Y.T., K.H.P., F.M., K.Y., S.H., M.N., C.J.F.B., A.T., Nagahama Study Group Visualization: Y.M. Supervision: C.J.F.B., A.T. Writing—original draft: Y.M., E.H.C.vD., M.M., M.N. Writing—review & editing: Y.H., A.I.dH., S.Y., A.M., L.J.C., J.A., A.T., K.M., S.N., C.B.H., D.S.C.N., L.P.C., H.C., T.K.N., C.P.P., K.J., T.S., Y.S., A.T., Y.T., K.H.P., F.M., K.Y., S.H., C.J.F.B., A.T., Nagahama Study Group.

Funding

Japan Society for the Promotion of Science (JSPS KAKENHI): JP17H04123 (YT), JP17H04126 (KA), JP17H04182 (KC), JP18K18450 (YT), JP19K17634 (SH), JP20H03841 (MM), JP25293141 (YT), JP26293198 (KC), and JP26670313 (YT). Japan Agency for Medical Research and Development (AMED): JP16dk0207006 (YT), JP16ek0109070 (FM), JP17ek0109196 (FM), JP17ek0210066 (HR), JP18ek0210096 (KC), JP18kk0205008 (FM), JP18le0110005 (YT), JP19ek0109283 (FM), JP19ek0210081 (YS), JP19le0110013 (YT), JP20dk0207027 (KT), JP20ek0109348 (FM), JP21ek0210116 (KC), JP21tm0724602 (YS), JP22dk0110040 (YT), JP22ek0210146 (YS), and JP22tm0724604 (YS). "Joint Usage/Research Center for Interdisciplinary Large-scale Information Infrastructures" and "High Performance Computing Infrastructure" in Japan: jh200047-NWH (MN), jh210018-NWH (MN), and jh220014 (MN). Takeda Medical Research Foundation (FM). Mitsubishi Foundation (YT). Daiwa Securities Health Foundation (YT). Sumitomo Foundation (YT). The sponsor or funding organization had no role in the design or conduct of this research.

Declarations

Competing interests

The authors declare no competing interests.

Additional information

Supplementary Information The online version contains supplementary material available at https://doi.org/10.1038/s41598-025-92210-6.

Correspondence and requests for materials should be addressed to M.M.

The Nagahama Study Group

Takeo Nakayama[21], Akihiro Sekine[22], Shinji Kosugi[23], Yasuharu Tabara[2,15] & Fumihiko Matsuda[2]

[21]Department of Health Informatics, Kyoto University School of Public Health, Kyoto, Japan. [22]Department of Infection and Host Defense, Graduate School of Medicine, Chiba University, Chiba, Japan. [23]Department of Medical Ethics/Medical Genetics, Kyoto University School of Public Health, Kyoto, Japan.